Ground-based Radar Detection of the inner Boundary of the Ion Plasma Sheet and its Response to the Changes in the Interplanetary Magnetic Field

P. T. Jayachandran[1], J. W. MacDougall[2], D. R. Moorcroft[2], and E. F. Donovan[3]

[1]Department of Physics, University of New Brunswick
Fredericton, New Brunswick, Canada

jaya@unb.ca

[2]Department of Physics, University of Western Ontario
London, Ontario, Canada

jmacdoug@uwo.ca / moorcrof@uwo.ca

[3]Department of Physics, University of Calgary
Calgary, Alberta, Canada

eric@phys.ucalgary.ca

ABSTRACT

SuperDARN is an array of HF radars, which covers most of the northern and southern high-latitude regions. The primary goal of this array is to study the dynamics of the large-scale convection pattern in order to understand the Solar wind – Magnetosphere- Ionosphere coupling (SW-M-I). Wide area coverage of the SuperDARN radars made it possible to detect some of the proxies for the magnetospheric land marks and boundaries on a global scale and shed some light on the on the some of the fundamental problems in the SW-M-I coupling process. One of the recent discoveries is that SuperDARN radar E region backscatter boundary in the dusk-midnight sector can be used as a proxy for the inner boundary of the ion plasma sheet. This discovery made it possible to study the boundary dynamics on a more global scale for the fist time. The boundary undergoes seasonal, diurnal, and substorm associated variations. One of the outstanding questions in the SW-M-I coupling research is how fast Magnetosphere-Ionosphere system reacts to the changes in the Interplanetary – Magnetic –Field (IMF). There are two schools of thoughts with regards to the changes in the ionospheric convection one being instantaneous and the other being delayed response. In this paper we present a study of the response of the equatorward boundary of the ion auroral oval on a global scale to the changes in the IMF. We have used the wide area coverage of the SuperDARN radar to investigate the response of the boundary to the changes in the upstream IMF. Estimation of the delay from the changes in the solar wind and IMF from an upstream satellite to the ionosphere is sometimes ambiguous. In order to avoid this ambiguity we have also used the changes in the central polar cap convection (both direction and speed) related to the changes in the IMF. This method also helps to precisely test the hypothesis of the fast and or slow changes. We will also compare the response of the ion auroral oval and the open/closed field line boundary detected using the ground based photometers in order to better understand the sequence of response from the changes in IMF to the changes in the polar cap convection, to the open/closed field line boundary and the equatorward boundary of the ion auroral oval.

Jayachandran, P.T.; MacDougall, J.W.; Moorcroft, D.R.; Donovan, E.F. (2006) Ground-Based Radar Detection of the Inner Boundary of the Ion Plasma Sheet and its Response to the Changes in the Interplanetary Magnetic Field. In *Characterising the Ionosphere* (pp. 21-1 – 21-12). Meeting Proceedings RTO-MP-IST-056, Paper 21. Neuilly-sur-Seine, France: RTO. Available from: http://www.rto.nato.int/abstracts.asp.

1.0 INTRODUCTION

The terrestrial magnetosphere is a reservoir of different charged particle populations of varying energy. The magnetic field-aligned guiding center motion of these charged particles is in general quasiperiodic between two mirror points. Numerous processes act on these particles that can lower the altitude of these mirror pints allowing the particles to interact collisionally with atmospheric neutrals and ions. These collisions leave the atmospheric atoms, molecules and ions in excited states (in the case of electron aurora). In the case of proton precipitation, the collisions often involve charge exchange, leaving the newly formed hydrogen atom in an excited state. Relaxation involves the emission of one or more characteristic photons, and the sum total of these emissions comprise the aurora.

We do not completely understand the scattering and acceleration mechanisms that lower the mirror heights of the particles causing them to "precipitate". Particle precipitation is an important source of energy which affects the electrodynamical properties, dynamics, thermal structures, as well as the constituent distribution in the high latitude ionosphere and thermosphere. The regions of intense auroral activity produced by these particle precipitations are called the "auroral oval". As stated above, the auroral oval represents the footprint of precipitating ions as well as electrons. Over the years most scientific effort went into the studies related to the electron part of the precipitating particles since in most regions it carries most of the energy. However, there are occasions when the proton (ion) precipitation carries significant part of the energy input into the Earth's upper atmosphere [1]. The cause of proton precipitation varies with magnetospheric regions and topology of the magnetic field lines [2 and references therein]. Proton precipitation is significant throughout the auroral oval and is often the dominant particle energy source in the cusp and at the equatorward boundary of duskside auroral oval [1,3,4]. Usually the dusk-midnight sector ion precipitation region maps to the inner ion plasma sheet and on average its earthward limit maps to the equatorward boundary of the ion auroral oval [4, 5,6,7,8]. The most equatorward boundary of the auroral oval in the dusk-midnight sector is the location where high energy ions stops precipitating (i.e. the transition between bounce trapping and strong pitch angle scattering). The equtorward cutoff of ion precipitation corresponds to both the ion isotropy and b2i boundaries [5,9,10] and this boundary also corresponds to the equatorward boundary of proton aurora [2]. This boundary represents an important transition in the magnetosphere and its location depends on the topology of the inner magnetosphere [2,8]. Since protons retain the large scale structure more efficiently than electrons, proton auroral measurements are an excellent probe for investigating magnetospheric substorms and Magnetosphere-Ionospheric (M-I) coupling process.

The most commonly used and reliable mean to measure the ion precipitation is the satellite based particle sensors used in the DMSP class of satellites [3]. The main disadvantage with the DMSP class satellite measurements, for the studies related to temporal and spatial dynamics of proton precipitation, is that the boundary is identified once during an oval crossing by the satellite, and hence no information about temporal evolution of the boundary is available on time scales less than typical times between crossings. Furthermore, the boundary is identified only on the satellite track, and so no information about the spatial structure of the boundary is obtained in this way. There are other techniques for determining the boundary and these techniques have its limitations.

Auroral signatures can be observed in most of the electromagnetic spectrum including the radiowaves. The association between the optical auroral forms and coherent radiowave backscatter in varying frequency ranges is well established [11,12,13,14,15,16] and these studies showed good temporal correlation between active optical auroral forms (associated with electron precipitation) and radiowave backscatter. Association between ion precipitation/proton aurora and coherent radiowave backscatter is not established until recently by Jayachandran et al., [17]. Jayachandran et al., [17] have discovered that in the dusk-midnight sector of the auroral oval there exists a type of E region HF backscatter associated with ion precipitation. Jayachanran et al., [17] used SuperDARN radar backscatter to show the association between E region backscatter in the dusk-midnight sector of the auroral oval and ion precipitation. SuperDARN [18] is an array of HF radars, which has wide area coverage and covers most of the northern and southern high-latitude regions. In the first section of the paper we outline the new ground-based radar technique to determine the boundary and in the section the new radar technique is applied to address one of the outstanding questions in the Solar Wind – Magnetosphere – Ionosphere (SW-M-I) research related to the response of the Magnetosphere – Ionosphere system to the changes in the Interplanetary Magnetic Field (IMF).

2.0 SUPERDARN RADAR TECHNIQUE TO DETERMINE THE EQUATORWARD BOUNDARY OF ION PRECIPITATION AND ITS VALIDATION WITH DIFFERENT MEASUREMENTS

SuperDARN radars [18] are deployed to study the large scale ionospheric convection pattern in the high latitudes. These radars presently cover much of the high-latitude regions of the northern and southern hemisphere. These pulsed radars operate in the frequency range of 8-20 MHz. The radar antenna system consists of a main array of 16 log periodic antennas and an additional array of 4 antennas (the interferometer array, which is used for elevation angle measurements). The antennas of each array are electronically phased with one another to form an antenna pattern in which the maximum gain (beam position) has one of 16 azimuthal pointing directions separated by ~3.2^o, distributed symmetrically about the radar boresite. This configuration will yield 16 beam directions for each of the radars and with 9 radars in the Northern hemisphere provides wide area coverage. SuperDARN was conceived of as a tool for monitoring convection on global scales. Figure 1 shows the location and area of coverage in the northern hemispheric radars, some of which are used for this study.

SuperDARN works on the principle of coherent backscatter from ionopsheric plasma irregularities generated by different irregularity mechanisms. Since SuperDARN radars operate in the HF frequency range the condition for backscatter (radar wave must be perpendicular to magnetic field) can be met at E and F regions of the ionosphere because of refraction and the elevation angle measured by the interferometer array will be crucial in determining the location of the radar backscatter echoes. Figure 2 shows the statistics of SuperDARN radar echoes detected by the Saskatoon SuperDARN radar during three months of 1997 along with the elevation angle measurements. Figure 2a shows the magnetic local time – magnetic latitude occurrence distribution of all the ionospheric echoes and Figure 2b shows corresponding elevation angle measurements. The echoes of interest to us the high-occurrence of near range echoes between 18:00-24:00 hrs local time. A close examination of the elevation angle reveals that these echoes are coming from low elevation angles and they are therefore E region echoes. A comparison of this figure with the ion precipitation statistics of ion precipitation using DMSP satellite particle measurements [1] reveals that the high concentration of these E region echoes corresponds to the region of high energy ion precipitation. Once the association between E region backscatter and ion precipitation is established the next logical step is to use this type of backscatter to determine the boundary of E region backscatter and see whether this boundary corresponds to any important particle boundaries.

Jayachandran et al., [6] compared the location of the equatorward boundary of SuperDARN E region backscatter with DMSP particle boundaries and concluded that the equatorward boundary of these E region backscatter corresponds to the b2i boundary (equatorward boundary of high energy ion precipitation). A later study [19] reached the same conclusion that equatorward boundary of radar backscatter corresponds to the equatorward boundary of ion precipitation in the dusk midnight sector. Jayachandran et al., [7] also compared

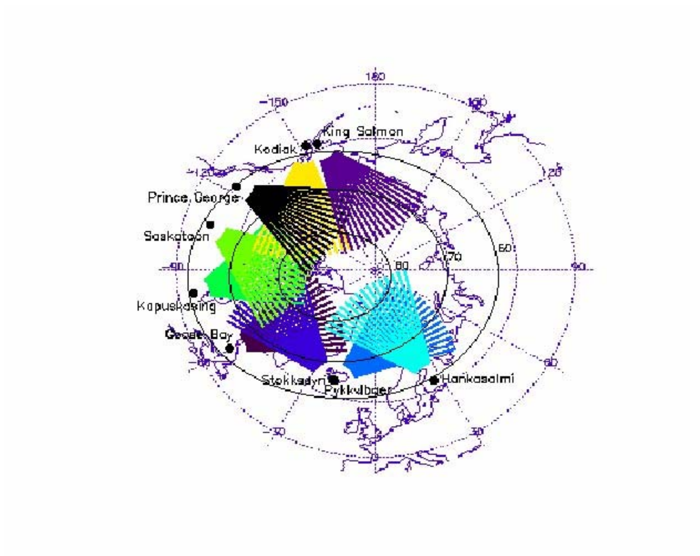

Figure 1: Location of the Northern hemisphere SuperDARN radars.

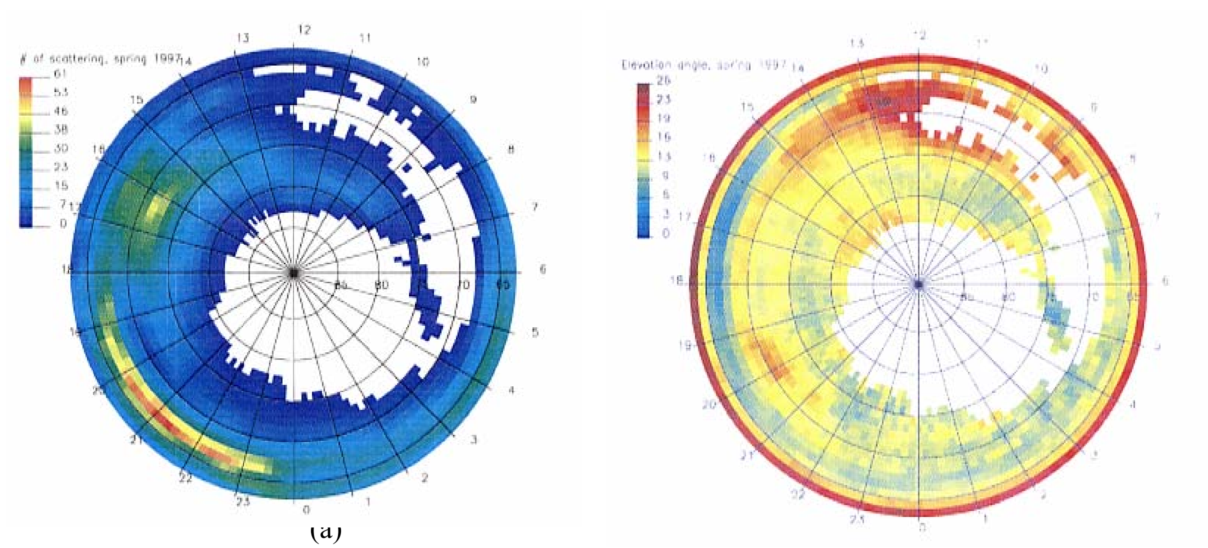

Figure 2: Magnetic latitude – Magnetic Local time distribution of the occurrence of (a) backscatter and (b) corresponding elevation angle for SuperDARN Saskatoon radar during three months of 1997.

the location of the radar backscatter boundary with the equatorward boundary determined using ground H_β measurements and concluded that the two boundaries corresponds well and shows that temporal behavior of these two boundaries follow each other very well. Figure 3 shows the distribution of the boundaries determined by the (a) radar, (b) DMSP Satellite, and (c) ground based Meridian Scanning photometer respectively. The mean and standard deviation for each distribution is given in each figures. Even though these are not simultaneous observation the distribution shows similar patterns and confirms earlier results [6,7,19] that in the dusk-midnight sector SuperDARN radar backscatter boundary can be used as a proxy for the b2i boundary. One factor to keep in mind is that the radar data used for this study has latitudinal limitations (lower limit of Mag. Lat. 62.5^{o}N due to the location of the radar and higher limit of 68.5^{o}N due to the maximum latitude of obtaining direct E region backscatter).

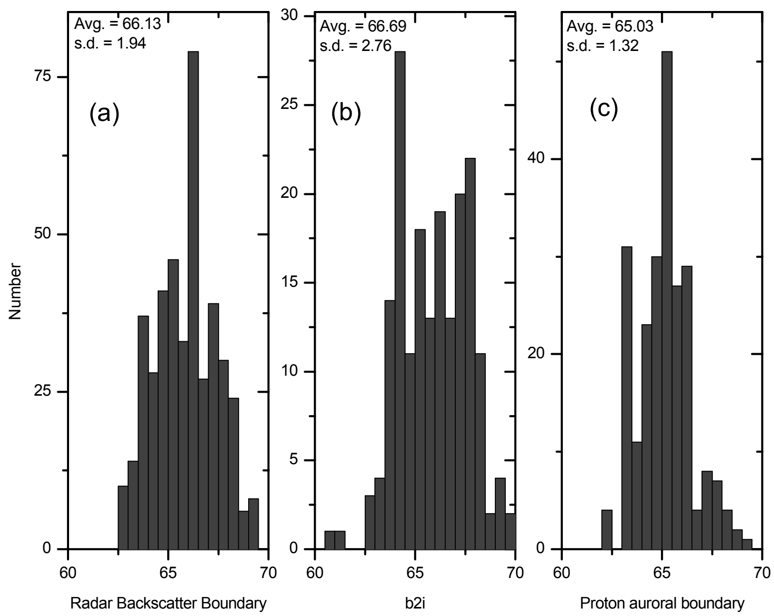

Figure 3: Distribution of the boundaries determined by (a) radar (b) DMSP satellite, and (c) H_β emission.

Association between E region backscatter and ion precipitation in the dusk-midnight sector can be linked with the plasma instability mechanism and the geometrical conditions for the radiowave backscatter. Since we are dealing with SuperDARN, which operates at HF, vertical gradients of the ionization play an even more important role in the generation of irregularities than at VHF [20]. The association of observed E region irregularities with proton aurora and high-energy ion precipitation suggests that these irregularities are formed through the gradient drift mechanism. The Hβ emissions are due primarily to several to tens of KeV precipitating CPS protons, which deposit most of their energy in the E region [21], and produce steep gradients in electron density. This gradient, and a properly directed electric field makes the E region unstable through the gradient drift instability mechanism and produces irregularities and thus radiowave backscatter. Generally, in the dusk - midnight sector of the auroral oval, the electric field is directed northward and the bottom side of the E region is unstable through the gradient drift instability mechanism. Further, the absence of E region backscatter if the Hβ intensity is < 20 R and the disappearance of the backscatter if the electric field changes its directions also confirm that the generation mechanism of these irregularities is the gradient drift instability.

It should be emphasized that other factors such as refraction and radar geometry (location) affects the detection of HF irregularities. This can have important consequence in the detection of E region backscatter and identification of the boundary. So far we have analysed the SuperDARN data from the Saskatoon, Kapuskasing and Goose Bay SuperDARN radars to identify the equatorward boundary of the auroral oval using the E region backscatter. Uspensky et al., [22] has also reported the presence of "ribbon echoes" (narrow region of E region backscatter) from the diffuse auroral region using the SuperDARN Finland radar. For the Finland radar, the geometry is different from other radars, the incident radar wave is almost perpendicular to the magnetic field (condition required for radio backscatter) without refraction, implying that refraction actually produces a negative effect (bends the ray away from perpendicularity). Hence the irregularities are detected only from the region where there is no refraction (region where the ray is orthogonal to the isoelectron density surface). This is in contrast to the Saskatoon, Kapuskasing, and Goose Bay radars for which the incident rays are a few degrees from the normal and refraction is necessary to obtain perpendicularity. A detailed study is required to determine which of the other SuperDARN radars (in northern and southern polar regions) can actually determine the auroral boundary taking all the factors into consideration.

3.0 BOUNDARY RESPONSE TO THE CHANGES IN THE INTERPLANETARY MAGNETIC FIELD

One of the outstanding questions in the SW-M-I coupling research is the time of response of the Magnetosphere-Ionosphere system to the changes in the IMF. There are two basic schools of thoughts based on the convection response to the changes in the IMF: Immediate response [23,24,25,26] and propagating response [26]. Recently several authors have reported a two stage response [27,28]. This is still an outstanding and controversial issue in the SW-M-I coupling research. One way to resolve this issue is to study the response of other parts of the M-I system to understand the consistencies/inconsistencies in the response time of the M-I system to the changes in the IMF. The method described in the previous section provides a new tool to address this issue. There are no studies in the literature that we are aware of related to the response of the equatorward boundary of the ion auroral oval to the changes in the IMF basically due to the lack of good temporal resolution boundary measurements. The new radar technique outlined above allowed us to study this important aspect of the SW-M-I coupling in detail. It is known that the during the southward IMF conditions there is significantly more energy input into the magnetosphere and the auroral oval expands equatorward. The technique described in the previous section provides very good temporal and spatial resolution measurements of the equtorward boundary of the ion auroral oval in the dusk-midnight sector and we are in position to make use of this technique to address the response of the boundary to the transition in the IMF.

For this part of the study we have used the solar wind measurements from the upstream solar wind monitoring WIND satellite. The solar wind measurements shown in this paper is corrected for the travel time from the solar wind monitor to the magnetopause using the method described by [27]. For the boundary response we have used SuperDARN radar measurements from the Saskatoon superDARN radar. For some events we have also used ground based Hβ measurements from GILLAM (67.47^{o} N Mag. Lat.) to determine the equtoarward boundary of the proton aurora as discussed by Donovan et al., [2] for cross checking the response. Figure 4 shows the time history of the measurements for an event of 24 March 2006 for the time interval 06-08 UT. Figure 4a shows the IMB Bz component (correct for the delay), Figure 4b shows the Latitude-Time-Velocity

(LTV) plot of the beam 4 (meridional beam) of the SuperDARN Saskatoon radar, and Figure 4c shows the Hβ keogram of Gillam Meridian Scanning Photometer (MSP). IMF predominantly northward till 06:20 UT and turned southward at ~06:20 UT. The equatorward boundary measured by the SuperDARN radar remained at constant latitude of ~66^{o} magnetic latitude till ~06:48 UT and started moving equatorward afterwards. The equatorwrd boundary of the proton aurora (white line on Figure 4c) also remained at constant latitude of 66o till ~06:48 UT and started moving equatorward afterwards. The estimated delay between the IMF transition at the magnetopause and the equatorward motion of the boundary is ~28 minutes. This example clearly shows the delayed response of the boundary to the IMF transition.

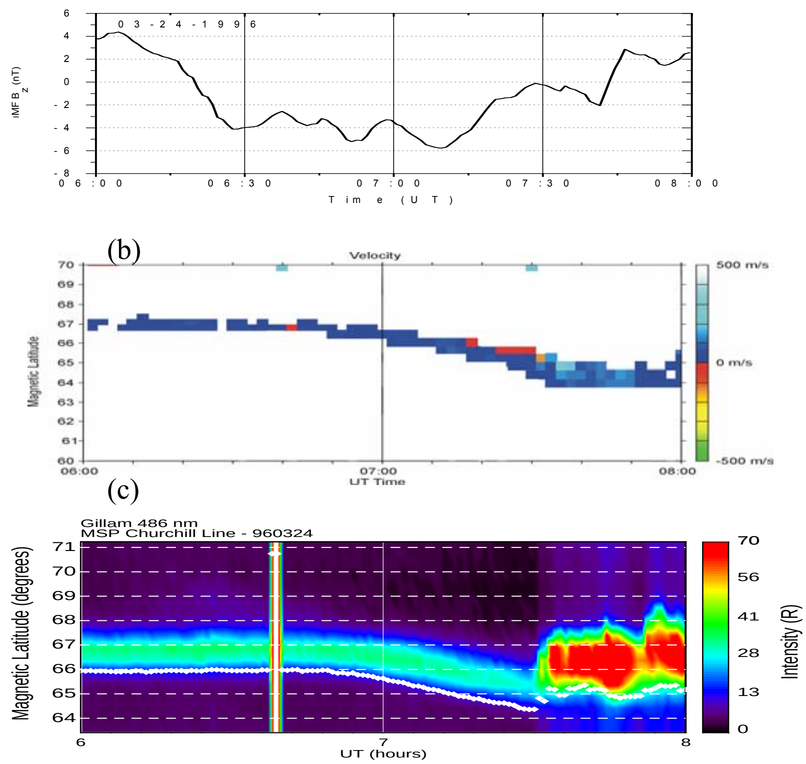

Figure 4: Variations of (a) IMF Bz, (b) Saskatoon SuperDARN radar backscatter velocity, and (c) Hβ emission intensity between 6-8 UT of 3 March 1996. All latitudes shown in the figure are magnetic latitudes.

Determination of the time of the IMF transition from the upstream solar wind monitor to the magnetopause is always ambiguous and there are different techniques for the estimation of the delay. Each of these methods yields different results [29]. In order to avoid this ambiguity one can use the ionospheric convection signatures associated with the IMF transition as a time marker of the arrival of the IMF changes in the ionosphere and determine the delay of the boundary response with respect to this convection features. Signatures of the polar cap convection changes associated with the North-South transition of the IMF are the change of the convection direction from sunward to antisunward direction and the increase of the convection speed [27,30]. For this purpose we have used convection measurements from a Canadian Advanced Digital Ionosonde (CADI) from a central polar cap station Eureka (88.67^{o}N Mag. Lat.). A typical example of the convection change measured at Eureka and boundary response detected by SuperDARN radar along with the IMF measurements for the time period 07-10 UT of 22 March 1997 is shown in Figure 5. Figure 5a shows the variation of IMF Bz, Figure 5b shows the convection speed, Figure 5c shows the convection direction, and

Figure 5d shows the RTV plot of SuperDARN Saskatoon radar. The solid and dashed line in Figure 5c represents the sunward and antisunward convection direction for Eureka. The IMF North-South transition occurred at the magnetopause at ~08: 06 UT and IMF was predominantly northward prior to this transition. The convection direction was predominantly in the sunward direction (due to the northward IMF condition) till ~08:14 UT and changed antisunward afterwards. The convection speed started increasing after ~ 08:14 UT responding to the N-S transition of the IMF. Prior to this the convection speed was very low due to the northward IMF condition. There is delay between the IMF transition and the convection response and is not a topic for this paper. We are taking this convection response in the polar cap is signature of the N-S transition of the IMF and estimating the delay of the boundary response from this reference time. From Figure 5d we can see that the location of the boundary was at constant latitude of 66.5^{o} between the interval 07:56 UT and 08:42 UT and afterward the boundary started moving equatorward. There was a delay of ~28 minutes from the convection change and the equatorward expansion of the boundary. We have anlaysed a total of 16 clear events and estimated delay the using the same method mentioned above and plotted the estimated delay distribution in Figure 6. The estimated delay varied between the range of 22-42 minutes with peak of distribution at ~27 minutes and the average of the distribution was ~30 minutes. This clearly shows the boundary always shows a delayed response to the N-S transition of the IMF.

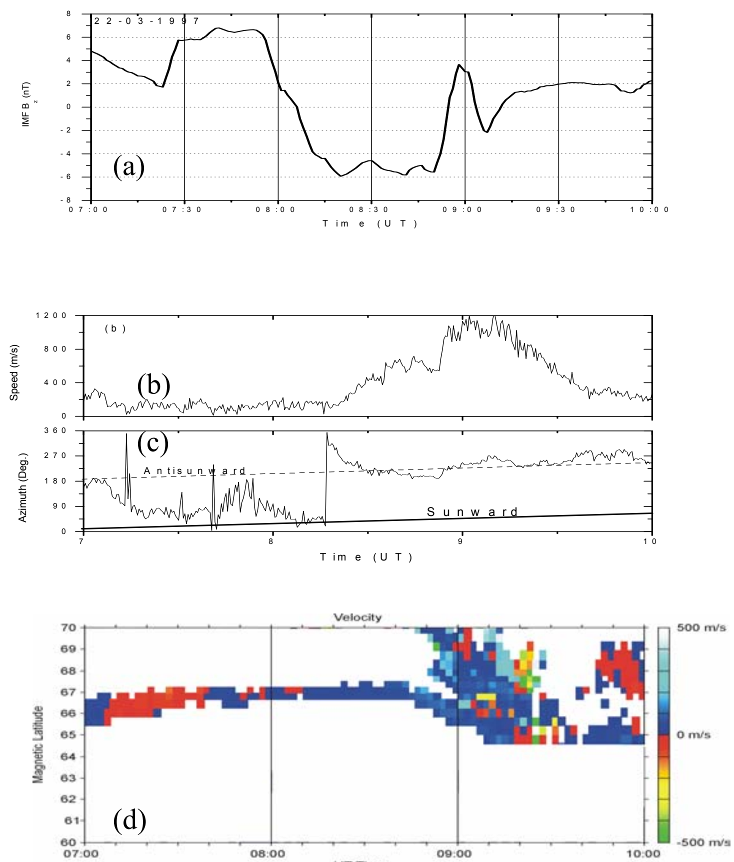

Figure 5: Variations of (a) IMF Bz, (b) convection speed, (c) convection direction, and (d) Saskatoon SuperDARN radar backscatter velocity between 6-8 UT of 22 March 1997. Convection measurements are made using Canadian Advanced Digital Ionosonde (CADI) measurements from Eureka. Solid and dashed line in the panel c of the figure represents the sunward and antisunward direction for Eureka respectively. All latitudes shown in the figure are magnetic latitudes.

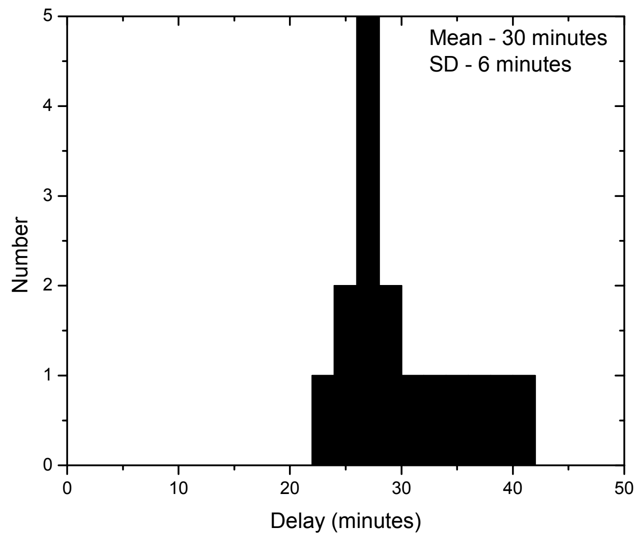

Figure 6: Distribution of estimated delay of the boundary response from the polar cap convection changes associated with the N-S transition of the IMF.

4.0 SUMMARY AND CONCLUSIONS

SuperDARN E region backscatter boundary can be used as a tracer of the equatorward boundary of the ion auroral oval in the dusk-midnight sector. The advantage of this technique is the high temporal and spatial resolution measurements of the boundary, which is crucial in understanding of the some of the fundamental processes in the SW-M-I coupling such as the response of the M-I system to the transitions in the IMF and auroral substorm process. The boundary always shows a delayed response to the transitions in the N-S transition of the IMF. The ambiguity in calculating the delay from the upstream solar wind monitor is avoided by using convection response in the polar cap to the transition of the IMF as a reference time. Estimated delay using this method also clearly showed the delayed response indicating that the delay is relay and not due to the ambiguity in the estimation of the delay from the upstream solar wind monitor to the magnetopause. A detailed study is required to understand the cause of the delay.

5.0 REFERENCES

[1] Galand, M., Fuller-Rowell, T.J. & Codrescu, M.V. (2001). Response *of the upper atmosphere to auroral protons*. J. Geophys. Res., 106,

[2] Donovan, E.F., Jackel, B.J., Voronkov, I., Sotirelis, R., Creutzberg, R., & Nicholson, N.A. (2003). *Ground-based optical determination of the b2i boundary: A basis for an optical MT-index*. J. Geophys. Res., 108, 1115, doi:10/1029/2001JA009198.

[3] Hardy, D.A., Gussenhoven, M.S., & Brautigam, D. (1989). *A statistical model of auroral ion precipitation*. J. Geophys. Res., 94, 370.

[4] Newell., P.T., Wing, S., Sotirelis, T., & Meng, C.I. (2005). *Ion aurora and its seasonal variations*. J. Geophys. Res., 110, Art. No. A01215.

[5] Newell, P.T., Sergeev, V.A., Bikkuzina, G.R., &. Wing, S. (1998). *Characterizing the state of the magnetosphere: Testing the ion isotropy boundary maxima latitude (b2i) and the ion isotropy boundary*. J. Geophys. Res., 103, 4739.

[6] Jayachandran, P.T., MacDougall, J.W., St-Maurice, J.-P., Moorcroft, D.R., Newell, P.T., & Prikryl, P. (2002). *Coincidence of the ion precipitation boundary with the HF E region backscatter boundary in the dusk-midnight sector*. Geophys. Res. Lett., 10.1029/2001GL014184.

[7] Jayachandran, P.T., Donovan, E.F., MacDougall, J.W., Moorcroft, D.R., St-Maurice, J.-P., & Prikryl, P. (2002). *SuperDARN E region backscatter boundary in the dusk-midnight sector-Tracer of the equatorward boundary of the auroral oval*. 20, 1899.

[8] Jayachandran, P.T., Donovan, E.F., MacDougall, J. W., et al. (2005). *Global and local equatorward expansion of the auroral oval before substorm onset*. J. Geophys. Res., 110, Art. No. A05204.

[9] Sergeev, V.A., Mitchell, D.G., Russell, C.T., & Williams, D.J. (1993). *Structure of the tail plasma current sheet at ~11RE and its changes in the course of a substorm*. J. Geophys. Res., 98, 17,345.

[10] Newell, P.T., Feldstein, Y.I., Galperin, Y.I., & Meng, C.I. (1996). *Morphology of nightiside precipitation.*. J. Geophys. Res., 101, 10,737.

[11] Herlofson, N. (1947). *Interpretation of radio echoes from polar aurora*. Nature,160, 867, 1947.

[12] Bates, H. F., Sharp, R.D., Belon, A.E., & Boyd, J.S. (1969). *Spatial relationship between HF radar aurora, optical aurora and electron precipitation.*, Plannet. Space. Sci., 17, 83.

[13] Romick, G.J., Ecklund, W.L., Greenwald, R.A., Balsley, B.B., & Imhof, W.L. (1974). *The relationship between the >130 KeV electron trapping boundary, the VHF radar backscatter, and the visual aurora*. J. Geophys. Res., 79, 2439.

[14] Moller, H.G. (1974). *Backscatter results from Lindau, II, The movements of curtains of intense irregularities in the polar F layer*. J. Atmos. Terr. Phys., 36, 1487.

[15] Hall, G.E., Moorcroft, D.R., Cogger, L.L., & Andre, D. (1990). *Spatial relationship between large aspect angle VHF radio aurora and 557.7 nm emissions: Evidence for refraction*. J. Geophys. Res., 95, 15,281.

[16] Milan, S.E., Lester, M., Sato, N., Takizawa, H., & Villain, J.-P. (2000). *Investigation of the relationship between optical auroral forms and HF radar E region backscatter.,* Ann. Geophysicae, 18, 608.

[17] Jayachandran, P.T., St-Maurice, J.-P., J. MacDougall, J.W., & Moorcroft, D.R. (2000). *HF detection of slow long-lived E region plasma structures*. J. Geophys. Res., 105, 2425.

[18] Greenwald, R.A., et al. (1995). *DARN/SuperDARN: A global view of high latitude convection*. Space. Sci., Rev., 71, 763.

[19] Sotirelis, T., J. Ruohoniemi, J.M., Barnes, R.J., et al. (2005). *Comparison of SuperDARN radar boundaries with DMSP particle precipitation boundaries*. J. Geophys. Res., 110, Art. No. A06302.

[20] St-Maurice, J.-P., Prikryl, P., Danskin, D.W., Hamza, A.M., Sofko, G.J., Koehler, J.A., Koustov, A.V., &. Chen, J. (1994). *On the origin of narrow non-ion-acoustic coherent radar spectra in the high-latitude E region*. J. Geophys. Res., 99, 6467.

[21] Vontrat-Reberac, R.., Fontaine, R.D., Blelly, P.L., & Galand, M. (2001). *Theoretical predictions of the effect of cusp and dayside precipitation on the polar ionosphere*. J. Geophys. Res., 106, 28,857.

[22] Uspensky, M., Eglitis, P., Opgenoorth, H., Starkov, G., Pulkkinen, T., & Pellinen, R. (2001). *On auroral dynamics observed by HF radar: 1. Equatorward edge of the afternoon-evening diffuse luminosity belt*. Ann. Geophysicae, 18, 1560.

[23] Shepherd, S.G., Greenwald, R.A., & Ruohoniemi, J.M. (1999). *A possible explanation for rapid, large scale ionospheric response to southward turning of the IMF*. Geophys. Res., Lett., 26, 3197.

[24] Ridley, A.J., Gang Lu, Clauer, C.R., & Papitashvili, V.O. (1998). *A statisticl study of the ionospheric responce chaning interplanetary magnetic field conditions using the assimilative mapping of ionospheric electrodynamic technique*. J. Geophys. Res., 103, 4023.

[25] Ridley, A.J., Gang Lu, Clauer, C.R., & Papitashvili, (1999). *Reply*. J. Geophys. Res., 104, 4393.

[26] Lockwood, M.J., & Coley, S.W.H. (1999). *Comment*. J. Geophys. Res., 4387.

[27] Jayachandran, P.T., & MacDougall, J.W. (2000). *Central polar cap convection response to short duration southward interplanetary magnetic field*. Ann. Geophys., 18, 887.

[28] Lu, G., Lummerzheim, D., Ruohoniemi, J.M., et al. *Ionospheric response to the interplanetary magnetic field southward turning: Fast onset and slow reconfiguration*. J. Geophys. Res., 107, Art. No. 1153.

[29] Ridley, A.J. (2000). *Estimation of the uncertainty in timing the relationship between magnetospheric and solar wind processes*. J. Atmos. Solar. Terr. Phys., 62, 757.

[30] Jayachandran, P.T., & MacDougall, J.W. (2001). *Sunward polar cap convection*. J. Geophys. Res., 106, 29009.

UNCLASSIFIED/UNLIMITED